Lightweight Dual-Reference Adaptive Change Detection for Robust UAV-Based Surveillance

Kamal Sandeep Karreddula*, Alok Kanti Deb

Abstract— **Unmanned Aerial Vehicle (UAV)-based surveillance systems commonly rely on continuous image processing or data-intensive detection methods, which are not suitable for resource-constrained onboard platforms. Lightweight dual-reference approaches, such as Difference of Difference (DoD) provides efficient change detection but suffers from fixed thresholds and static reference models, making them sensitive to illumination variations and gradual environmental changes. This paper presents a Lightweight Dual-Reference Adaptive Change Detection (DRACD) method for robust UAV-based surveillance. The proposed method extends the conventional dual-reference formulation by incorporating adaptive thresholding and a rolling reference update mechanism, enabling dynamic adjustment to environmental variations while preserving computational efficiency. The approach operates using pixel-wise difference operations, making it suitable in real-time implementation. Experimental evaluation using imagery captured from a F450 quadcopter demonstrates that the proposed method effectively suppresses false alarms caused by illumination changes while maintaining reliable detection of abnormal events. The results further demonstrate clear and consistent separation between normal and abnormal conditions across varying environmental scenarios.**

***Keywords*: Dual-Reference Change Detection (DRACD), Adaptive Thresholding, Visual Surveillance, UAV Surveillance, Embedded Systems, Real-Time Decision Making**

I. Introduction

Unmanned Aerial Vehicles (UAVs) have become a key platform for aerial surveillance due to their mobility, flexible deployment, and ability to capture high-resolution imagery in challenging environments such as borders, disaster zones, and critical infrastructure monitoring [1], [2]. However, most UAV-based surveillance systems rely on continuous video acquisition and frame-by-frame processing using classical computer vision or deep learning techniques [3]–[6]. These approaches impose significant computational demands and are often not suitable for resource-constrained onboard platforms.

Traditional object detection methods, including convolutional neural networks and feature-based techniques, require large training datasets and high computational resources [7], [8]. While these methods achieve high detection accuracy, their deployment in UAV systems is limited by domain dependency and real-time processing constraints. Background subtraction and frame differencing methods provide lightweight alternatives; however, their performance degrades in UAV scenarios due to camera motion, illumination variations, and dynamic backgrounds [9]–[11].

Kamal Sandeep Karreddula is a Research Scholar in the Department of Electrical Engineering at the Indian Institute of Technology, Kharagpur, 721302 INDIA (e-mail: kamal.sandeep.zes@gmail.com).

Alok Kanti Deb is a Professor in the Department of Electrical Engineering at the Indian Institute of Technology, Kharagpur, 721302 INDIA (e-mail: alokkanti@ee.iitkgp.ac.in).

To address these challenges, lightweight change detection approaches based on reference image comparison have been explored. In particular, a dual-reference Difference of Difference (DoD) method [12] has been presented for UAV-based surveillance, offering a computationally efficient approach suitable for embedded implementation. The method performs effectively under relatively stable conditions, particularly in planar environments where scene variations due to illumination and minor positional drift remain limited. However, such methods rely on fixed thresholds and static reference images, which limits their ability to adapt to gradual environmental variations.

In complex environments involving structures such as buildings, vegetation, and non-uniform backgrounds, environmental variations introduce significant deviation, reducing the reliability of fixed-threshold formulations. Since the threshold remains fixed after calibration, the method cannot adapt to gradual environmental changes such as illumination variation, seasonal changes, and minor viewpoint shifts. As a result, variations unrelated to actual intrusions may lead to false alarms or missed detections, reducing reliability during long-duration surveillance. These limitations highlight the need for adaptive mechanisms that can dynamically adjust to changing scene conditions.

To overcome these limitations, this paper presents a lightweight Dual-Reference Adaptive Change Detection (DRACD) method for robust UAV-based surveillance. The proposed approach extends the conventional dual-reference formulation by incorporating adaptive thresholding and a rolling reference update mechanism. These enhancements enable dynamic adjustment to environmental variations, unlike fixed-threshold methods, while maintaining computational efficiency comparable to conventional approaches.

The effectiveness of the proposed method is validated using imagery captured from a F450 quadcopter [13] under varying environmental conditions. Experimental results demonstrate improved robustness to illumination changes and clear separation between normal and abnormal conditions, while preserving lightweight computational characteristics suitable for real-time embedded deployment.

The main contributions of this work are summarized as follows:

- A lightweight DRACD method for UAV-based surveillance that improves robustness to environmental variations while maintaining computational efficiency.
- An adaptive thresholding mechanism that dynamically adjusts to environmental variations, improving robustness to illumination changes.
- A rolling reference update strategy that maintains stability while preventing drift during long-duration surveillance.
- Experimental validation on real-world UAV imagery demonstrating clear separation between normal and abnormal conditions.

The remainder of this paper is organized as follows. Section II reviews related work in UAV-based change detection. Section III presents the proposed DRACD method, including adaptive thresholding and the rolling reference update mechanism. Section IV describes the experimental setup and evaluation methodology. Section V presents the results and discussion. Finally, Section VI concludes the paper.

II. Related Work

Change detection and object detection for UAV-based surveillance have been widely studied using both data-driven and classical approaches. Deep learning-based methods, including convolutional neural networks and single-stage detectors such as You Only Look Once (YOLO) and Single Shot MultiBox Detector (SSD), have demonstrated high accuracy in detecting objects in aerial imagery [3]–[6]. However, these methods require large annotated datasets and significant computational resources, limiting their suitability for real-time deployment on resource-constrained UAV platforms [7].

To address computational constraints, several efficient approaches have been explored. Background subtraction and frame differencing techniques are commonly used for detecting motion in surveillance systems [9], [10]. While these methods are computationally efficient, their performance degrades significantly in aerial situations due to camera motion, dynamic backgrounds, and illumination variations [11]. These limitations make them unreliable for long-duration aerial surveillance.

Reference-based change detection methods provide an alternative approach by comparing current observations with previously captured images. Such methods reduce redundant processing by focusing only on scene variations. A dual-reference DoD formulation has been presented for UAV-based surveillance, where deviation between reference images and surveillance observations is compared against a threshold determined during calibration [12]. While computationally efficient, the method assumes stable baseline variation and relies on fixed thresholds and static references. As a result, the method is sensitive to environmental variations and may produce incorrect detections under changing illumination or minor viewpoint variations.

In environments with structural complexity, illumination variation, and minor viewpoint changes, these assumptions lead to increased deviation and incorrect detection. The lack of adaptation to such variations motivates the need for adaptive change detection methods that maintain computational efficiency while improving robustness to environmental variations. These limitations form the basis for the proposed adaptive dual-reference approach presented in this work.

III. Proposed Dual-Reference Adaptive Change Detection Method

This section presents the proposed Dual-Reference Adaptive Change Detection (DRACD) method for UAV-based surveillance. The method extends the conventional dual-reference formulation by incorporating adaptive thresholding and a controlled rolling reference update mechanism. These enhancements enable improved robustness to environmental variations while maintaining computational efficiency suitable for real-time embedded implementation.

Compared to the conventional dual-reference method [12], the proposed approach integrates deviation analysis with conditional threshold adaptation and controlled reference updates applied only under normal conditions, improving robustness while preventing drift during abnormal events.

A. Overview of Dual-Reference Change Detection

Dual-reference change detection method [12] utilize multiple reference images to capture normal variations in a scene. By comparing a current observation with reference images acquired under normal conditions, it becomes possible to identify deviations associated with abnormal events.

Let I_1 and I_2 denote two reference images captured under normal conditions at different time instances. The baseline deviation between the reference images is defined as:

$$D_b = |I_1 - I_2| \tag{1}$$

Given a surveillance image I_s, the deviation with respect to the reference image I_2 is computed as:

$$D_s = |I_s - I_2| \tag{2}$$

The final deviation is obtained as:

$$D_{fs} = |D_s - D_b| \tag{3}$$

Since D_{fs} is computed as a pixel-wise difference image, a scalar decision value is obtained by aggregating pixel intensities. In this work, D_{fs} is defined as the sum of absolute pixel differences over the entire image:

$$D_{fs} = \sum_{i=1}^{M} \sum_{j=1}^{N} |D_s(i,j) - D_b(i,j)| \tag{4}$$

where M and N denote the image dimensions.

This scalar formulation enables direct comparison with the adaptive threshold and separates natural variations from abnormal changes by subtracting baseline deviation.

B. Limitation of Static Dual-Reference Formulation

In conventional dual-reference approaches, the decision is made by comparing the final deviation D_{fs} with a threshold determined during calibration. Since the threshold remains fixed and reference images are not updated, the method cannot adapt to gradual environmental changes.

As a result, variations such as illumination changes or minor viewpoint shifts may significantly alter D_s, leading to incorrect detection. This limitation reduces reliability in long-duration UAV-based surveillance.

To address the limitations of the static dual-reference formulation, the overall workflow of the proposed adaptive change detection method is illustrated in Fig. 1.

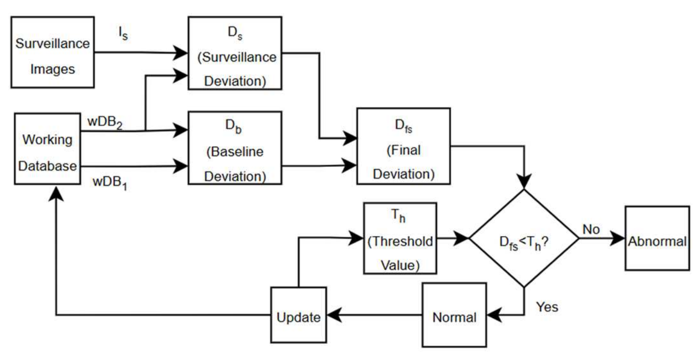

Fig. 1. Overview of the DRACD-based adaptive change detection process.

As shown in Fig. 1, the method utilizes dual-reference images to compute baseline deviation, which captures natural scene variations. The surveillance image is compared with the reference to obtain the final deviation, which is evaluated using an adaptive threshold. Based on the detection outcome, the threshold and reference images are updated dynamically under normal conditions, enabling continuous adaptation to environmental changes while preserving stability during abnormal events.

C. Adaptive Threshold Initialization (Calibration Stage)

To improve robustness, an adaptive threshold is initialized using calibration data.

Let I_t denote a calibration image captured under normal conditions. The deviation is computed as:

$$D_t = |I_t - I_2| \tag{5}$$

The calibration deviation is defined as:

$$D_{ft} = |D_b - D_t| \tag{6}$$

The initial adaptive threshold is defined as:

$$T_h^{(0)} = (1+\epsilon)D_{ft} \tag{7}$$

where, ϵ is a tolerance factor that accounts for natural variations such as illumination and minor viewpoint changes.

D. Online Adaptive Change Detection

During surveillance, the working reference images $wDB_1^{(n)}$and $wDB_2^{(n)}$ are initialized from DB_1 and DB_2, respectively. At each time step (n), the current observation $I_s^{(n)}$ is processed as follows.

The baseline deviation is computed as:

$$D_b^{(n)} = |wDB_1^{(n)} - wDB_2^{(n)}| \tag{8}$$

The surveillance deviation is defined as:

$$D_s^{(n)} = |I_s^{(n)} - wDB_2^{(n)}| \tag{9}$$

The final deviation is computed as:

$$D_{fs}^{(n)} = |D_s^{(n)} - D_b^{(n)}| \tag{10}$$

The deviation $D_{fs}^{(n)}$ represents the excess change beyond natural scene variation captured by $D_b^{(n)}$. This formulation prevents direct comparison with a single reference and instead evaluates relative deviation, improving robustness under varying environmental conditions.

An anomaly is detected when:

$$D_{fs}^{(n)} > T_h^{(n-1)} \tag{11}$$

where, $T_h^{(n-1)}$ is the adaptive threshold obtained from the previous update step.

This formulation isolates abnormal changes by removing baseline variations.

E. Adaptive Threshold Update

The threshold is dynamically updated under normal conditions as:

$$T_h^{(n)} = \begin{cases} (1+\epsilon)D_{fs}^{(n)}, & \text{if } (1+\epsilon)D_{fs}^{(n)} \geq T_h^{(n-1)} \text{(under normal)} \\ T_h^{(n-1)}, & \text{otherwise} \end{cases} \tag{12}$$

The adaptive threshold formulation is based on the assumption that the observed deviation $D_{fs}^{(n)}$ under normal conditions represents the upper bound of expected scene variations caused by illumination changes, sensor noise, and minor environmental disturbances. The multiplicative factor $(1+\epsilon)$ introduces a tolerance margin to accommodate small variations beyond the observed deviation, thereby maintaining separation between normal and abnormal conditions.

From a practical perspective, this formulation ensures stable adaptive behavior by dynamically adjusting the threshold according to scene variations. However, due to its non-decreasing nature, the threshold may become conservative under prolonged environmental changes, improving robustness against transient fluctuations while potentially reducing sensitivity to gradual scene evolution.

If an abnormal condition is detected, the threshold remains unchanged. This update mechanism ensures gradual adaptation to normal variations while maintaining stability and preventing model drift.

F. Rolling Reference Update Mechanism

To maintain an updated representation of the scene, the reference images are updated using a rolling mechanism:

$$\begin{aligned} wDB_1^{(n+1)} &= wDB_2^{(n)} \\ wDB_2^{(n+1)} &= I_s^{(n)} \end{aligned} \tag{13}$$

The update is performed only when the scene is classified as normal. During abnormal conditions, updates are skipped to preserve the last valid reference state. This mechanism ensures stability while enabling adaptation to slow environmental changes and reducing the possibility of incorporating abnormal changes into the reference model.

G. Algorithm Summary

The DRACD procedure is summarized as follows:

Algorithm 1: DRACD-Based UAV Surveillance Procedure

For each reference point (RP):

I. Capture surveillance image I_s

II. Compute: (8)–(10)

$D_b^{(n)} = |wDB_1^{(n)} - wDB_2^{(n)}|$,

$D_s^{(n)} = |I_s^{(n)} - wDB_2^{(n)}|$,

$D_{fs}^{(n)} = |D_s^{(n)} - D_b^{(n)}|$

III. Decision and update:

- If $D_{fs}^{(n)} > T_h^{(n-1)}$: trigger advanced detection and skip the update step for the threshold and working databases
- Else:

  update the adaptive threshold:

  $$T_h^{(n)} = \begin{cases} (1+\epsilon)D_{fs}^{(n)}, & \text{if } (1+\epsilon)D_{fs}^{(n)} \geq T_h^{(n-1)} \text{(under normal)} \\ T_h^{(n-1)}, & \text{otherwise} \end{cases}$$

  and update working databases

  $wDB_1^{(n+1)} = wDB_2^{(n)}, wDB_2^{(n+1)} = I_s^{(n)}$

The proposed method is computationally efficient due to its pixel-level operations and is suitable for real-time implementation on embedded platforms.

H. Method Characteristics

Compared to conventional change detection methods such as background subtraction [7], [8], the proposed DRACD method does not rely on explicit background modeling. The dual-reference formulation captures natural scene variability, while the adaptive thresholding and controlled update mechanism enable stable operation under varying environmental conditions.

The simplicity of the method, based on pixel-level operations, makes it suitable for real-time implementation on resource-constrained embedded platforms.

Compared to conventional dual-reference change detection methods, the proposed DRACD approach introduces two key differences. First, the decision threshold is adaptively updated based on the observed deviation, enabling dynamic adjustment to environmental variations rather than relying on a fixed calibration value. Second, the reference images are updated using a controlled rolling mechanism applied only under normal conditions, preventing drift during abnormal events. These modifications improve robustness while preserving the computational simplicity of the original dual-reference formulation.

Unlike fixed-threshold dual-reference methods, the proposed approach dynamically adapts to environmental variations while maintaining stability during abnormal events.

IV. Experimental Setup and Evaluation Methodology

A. UAV Platform and Implementation

The experimental evaluation is conducted using a quadcopter-based UAV platform equipped with an onboard embedded processing unit. The UAV is built on an F450 frame, as shown in Fig. 2 and utilizes a Pixhawk 4 [14] flight controller for stabilization and waypoint navigation. A Raspberry Pi (RPi) 3B+ is integrated as a companion computer to execute the proposed DRACD algorithm in real time [15]. Image acquisition is performed using an OV5647 camera module [16].

To ensure consistent ground coverage and reliable pixel-to-distance mapping, the UAV operates at a fixed altitude during all experiments. Image processing is performed entirely onboard using pixel-wise operations, enabling real-time execution without the need for specialized hardware acceleration. This setup allows the system to function autonomously in surveillance scenarios without reliance on external computation resources.

The experiments are conducted under hovering flight conditions, where the UAV maintains a fixed altitude and stable orientation during image acquisition at predefined surveillance points. Minor positional drift and small viewpoint variations may occur due to environmental factors; however, these are partially accommodated by the tolerance margin in the adaptive threshold formulation.

B. Data Acquisition and Experimental Conditions

Images are captured at predefined surveillance locations under controlled and real-world conditions. At each location, two reference images are acquired under normal conditions to initialize the dual-reference model. The experimental scenarios are categorized into three conditions: (i) Baseline condition: Static environment without any change, (ii) Environmental variation: Gradual illumination changes and minor scene variations, and (iii) Abnormal condition: Presence of intruding objects or persons.

These conditions are designed to evaluate both the robustness of the method to environmental variations and its ability to detect actual anomalies.

The evaluated environments represent diverse real-world surveillance conditions, including structured scenes and planar field environments under varying viewpoints. The dataset is intended to validate the practical effectiveness of the proposed method under representative UAV surveillance scenarios.

C. Parameter Configuration

The tolerance parameter ϵ is used to control the sensitivity of the adaptive threshold. The value of ϵ is determined empirically through repeated calibration under normal conditions. Experimental observations indicate:

(i) $\epsilon < 5\%$ results in frequent false alarms due to sensitivity to minor variations.

(ii) $\epsilon > 15\%$ reduces sensitivity to abnormal events.

(iii) $5\% < \epsilon < 15\%$ provides a balance between robustness and detection sensitivity. In this work $\epsilon = 10\%$ chosen across all experiments provides robustness and detection sensitivity.

D. UAV System Configuration

The UAV platform is composed of lightweight and commercially available components to ensure ease of deployment and real-time operation. The detailed hardware configuration of the UAV platform is summarized in Table I, while the corresponding system specifications are presented in Table II.

The UAV operates at a low-altitude flight profile to ensure consistent ground resolution for surveillance tasks. The propulsion system is configured to provide sufficient thrust for stable operation, while the onboard computing unit supports real-time image processing within the available power and weight constraints.

The system achieves a flight duration of approximately 15 minutes under nominal operating conditions. Images are captured at a resolution of 320 × 240, providing an effective trade-off between computational efficiency and sufficient scene detail required for deviation-based change detection. At the operating altitude, this resolution provides adequate representation of human-scale objects for deviation-based detection.

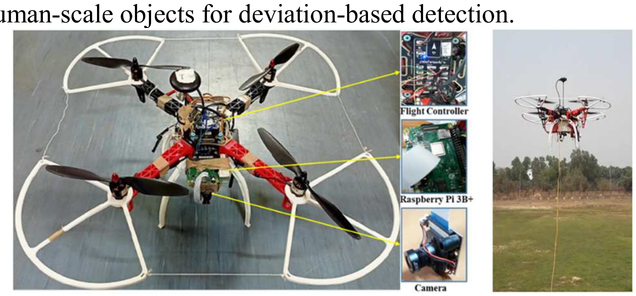

a b

Fig. 2. Quadcopter [13] system used for experimentation: (a) F450-based hardware, (b) UAV during flight testing.

TABLE I. COMPONENTS OF QUADCOPTER (UAV) SYSTEM

Component	Model
Frame	F450
Flight controller	Pixhawk 4
BLDC Motor	2212 (935 KV)
Propeller	1045 (10 inch)
Battery	LiPo 5200 mAh
Companion computer	Raspberry Pi 3B+
Camera	OV5647

TABLE II. SPECIFICATIONS OF THE DESIGNED SYSTEM

Characteristics	Values
System total weight	1570 gm
Net thrust	3440 gm
Thrust : Weight	2.2
Flight time	15 min
Operating Altitude	5 m
Image Resolution	320 × 240

E. Decision Metrics

To evaluate the performance of the proposed DRACD method, the following decision metrics are considered:

(i) False Alarm Rate (FAR): Measures the proportion of normal conditions incorrectly classified as abnormal. This metric is critical for assessing robustness under environmental variations.

(ii) Detection Accuracy: Represents the proportion of correctly classified normal and abnormal cases over the total number of observations.

(iii) Deviation Separation: Difference between the final deviation D_{fs} values corresponding to normal and abnormal conditions. This metric indicates the clarity of distinction between the two classes.

(iv) Precision: Measures the proportion of abnormal detections that are correctly identified.

(v) Recall: Measures the proportion of actual abnormal conditions correctly detected.

(vi) F1-Score: Harmonic mean of Precision and Recall, representing balanced detection performance.

These metrics collectively evaluate both the reliability and robustness of the proposed method under varying environmental conditions. The performance metrics are computed based on classification outcomes, including true positives, true negatives, false positives, and false negatives.

F. Implementation Details

The DRACD algorithm is implemented using grayscale images to reduce computational complexity. All operations are based on pixel-wise absolute difference calculations, ensuring low computational overhead.

The system operates sequentially, where images are captured and processed at each surveillance location. The adaptive threshold and rolling reference update mechanisms are applied dynamically during operation, enabling continuous adaptation to environmental changes while maintaining stability.

V. Results and Discussion

A. Illumination Robustness Analysis

Environmental variations, particularly illumination changes, significantly affect pixel intensities and often lead to incorrect detections in static threshold-based methods. This section evaluates the robustness of the proposed method under such variations.

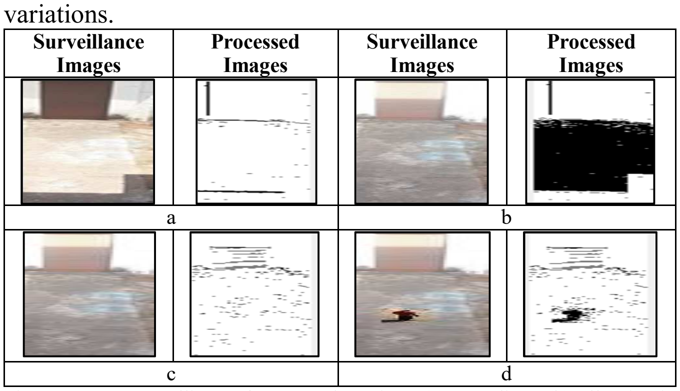

Fig. 3. DRACD rolling reference adaptation: (a) Baseline, (b) Illumination variation, (c) Rolling reference image update under normal condition, and (d) Abnormal condition (intruder).

The processed images shown in this section correspond to normalized deviation maps derived from the computed $D_{fs}^{(n)}$ values, where higher intensity regions indicate significant scene changes. Fig. 3 illustrates that rolling updates improve illumination robustness by adapting the working reference update under normal conditions, thereby reducing false alarms while preserving true anomaly detection. When an actual intruder is present, the deviation again exceeds the threshold (T_h), enabling correct abnormal detection. This behavior demonstrates that the proposed method effectively distinguishes environmental variations from true anomalies.

TABLE III. EFFECT OF ILLUMINATION VARIATION

Surveillance Condition	D_{fs}	T_h	**Detection**
Baseline (Normal)	88	97	Normal
Normal: Illumination change	7169	97	Abnormal
Normal: Rolling reference	65	97	Normal
Abnormal	228	97	Abnormal

A significant increase in deviation is observed under illumination change, where D_{fs} rises from 88 to 7169, exceeding the threshold and resulting in a false alarm. After applying adaptive thresholding and rolling reference updates under normal conditions, the deviation stabilizes to 65, which falls below the updated threshold, leading to correct classification.

B. Real-World Detection Performance

The proposed method is validated using imagery captured from a F450 quadcopter under varying environmental conditions. For qualitative evaluation, representative results from seven scenes are shown in Fig. 4, including structured environments (I–IV) and planar field environments (V–VII). The scenes are captured from front view, angled view, and top-view perspectives, enabling assessment across different geometries, viewpoints, and background conditions. Each column corresponds to a scene (I–VII), while rows (a)–(e) denote permanent database images, normal-condition images, their processed outputs, abnormal-condition images, and their processed outputs, respectively.

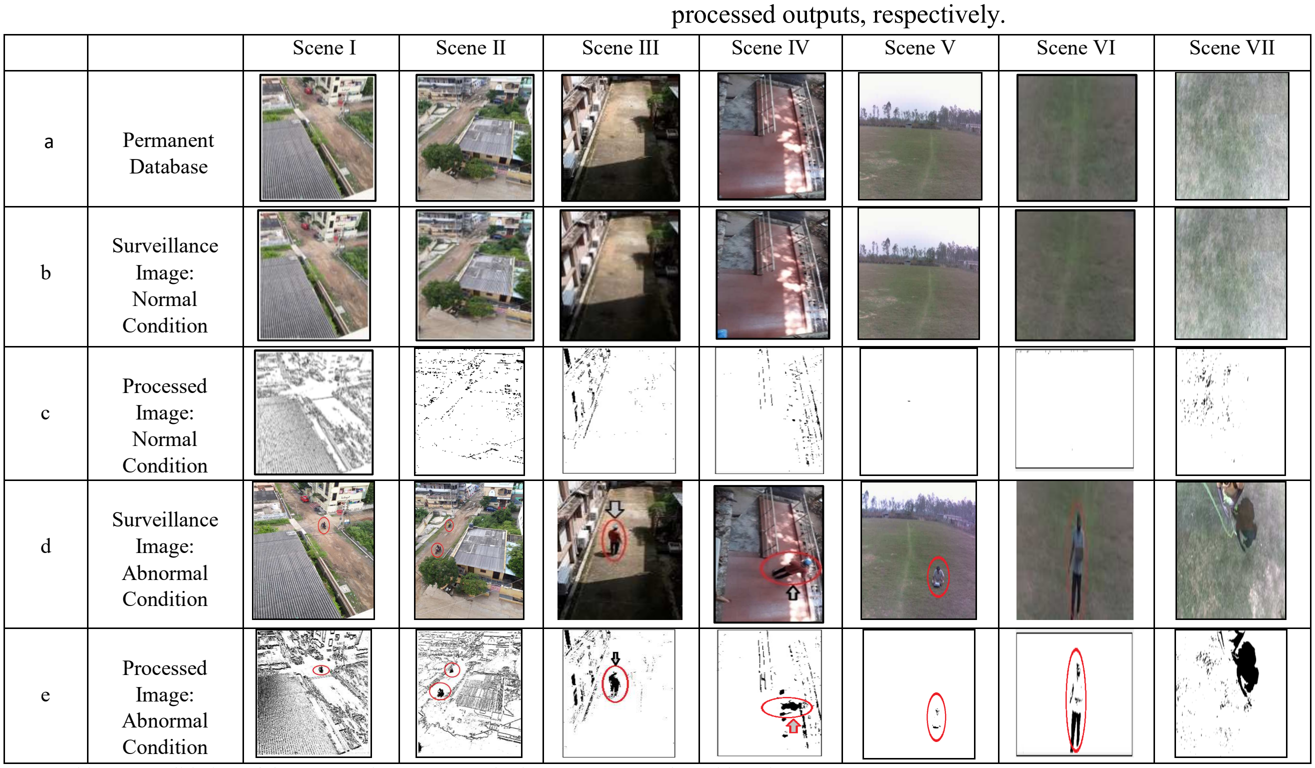

Fig. 4. Multi-scene validation of the proposed DRACD method across seven real-world environments

As shown in Fig. 4, the method suppresses environmental variations while highlighting abnormal regions. Normal scenes show minimal residual changes, whereas abnormal conditions produce distinct localized deviations corresponding to intrusions.

TABLE IV. MULTI-SCENE VALIDATION RESULTS USING DRACD ACROSS DIFFERENT REAL-WORLD ENVIRONMENTS

Scene	Ground Truth Condition	D_{fs}	T_h	Detection	Rolling Update
I	No intruder	57	60	Normal	Yes
I	Intruder	1049	63	Abnormal	No
II	No intruder	89	95	Normal	Yes
II	Intruder	1923	98	Abnormal	No
III	No intruder	632	695	Normal	Yes
III	Intruder	3203	655	Abnormal	No
IV	No intruder	597	636	Normal	Yes
IV	Intruder	3843	666	Abnormal	No
V	No intruder	26	30	Normal	Yes
V	Intruder	206	30	Abnormal	No
VI	No intruder	60	70	Normal	Yes
VI	Intruder	973	70	Abnormal	No
VII	No intruder	333	350	Normal	Yes
VII	Intruder	17695	367	Abnormal	No

The ground truth condition indicates the actual scene status, while the detection column represents the output of the proposed method. Table IV summarizes the quantitative surveillance results across real-world environments, including adaptive thresholds and rolling updates.

The results demonstrate consistent behavior across all environments. Under normal conditions, the deviation D_{fs} remains below the adaptive threshold, allowing correct classification and enabling rolling updates. In contrast, under abnormal conditions, the deviation significantly exceeds the threshold, resulting in accurate anomaly detection while preventing updates. This consistent separation confirms the robustness of the method across diverse environments.

C. *False Alarm Suppression Performance*

The ability to suppress false alarms under environmental variations is evaluated using multiple normal-condition observations. This analysis focuses specifically on normal scenes to assess the system's susceptibility to false alarms under varying environmental conditions. The results are summarized in Table V.

TABLE V. FALSE ALARM ANALYSIS

Scenario	Scene Type	Total Normal Cases	False Alarms	FAR (%)
Without adaptation	Planar	30	3	10
	Complex	20	10	50
With proposed method	Planar	30	1	3.33
	Complex	20	2	10

As shown in Table V, false alarm susceptibility varies significantly across scene conditions. Without adaptation, FAR increases from 10% in planar scenes to 50% in complex scenes due to environmental variability. With the proposed adaptive mechanism, FAR is reduced to 3.33% and 10%, respectively, demonstrating improved stability and reliability under challenging conditions.

D. *Quantitative Performance Comparison*

While Table V evaluates false alarm suppression under normal conditions, the overall detection performance across both normal and abnormal scenarios is presented in Table VI. The proposed method is compared with classical lightweight change detection techniques including frame differencing, background subtraction, and the conventional dual-reference (DoD) method [17], [18].

The results in Table VI are obtained using surveillance images collected across seven real-world environments under varying environmental conditions, as illustrated in Fig. 4. The evaluation dataset consists of 50 images including both normal and abnormal conditions. The dataset includes representative structured and planar environments to evaluate practical UAV surveillance performance.

The computational time per frame is measured on a RPi 3B+ platform using input images of size 320 × 240, confirming suitability for real-time deployment.

TABLE VI. PERFORMANCE COMPARISON WITH BASELINE METHODS

Method	Accuracy (%)	Precision %	Recall %	F1-Score %	FAR (%)	Time per Frame (s)
Frame Differencing [17]	72	74	68	71	24	0.020
Background Subtraction [17]	80	80	80	80	20	0.071
DoD [12]	86	85	88	86	16	0.032
DRACD	92	92	92	92	8	0.035

As shown in Table VI, frame differencing and background subtraction produce higher false alarm rates due to illumination sensitivity. The dual-reference DoD method improves stability but remains limited by fixed thresholds. In contrast, DRACD achieves 92% accuracy with an 8% false alarm rate, effectively distinguishing abnormal events from normal environmental variations. Precision, Recall, and F1-score values further confirm the improved detection reliability and robustness of the proposed DRACD method under varying environmental conditions.

E. *Comparative Analysis*

The proposed method is compared with the conventional dual-reference approach in terms of thresholding, adaptability, false alarm behavior, and robustness, as summarized in Table VII.

TABLE VII. COMPARATIVE ANALYSIS OF DETECTION METHODS

Method	Threshold Type	Adaptation	False Alarm Behavior	Robustness
DoD [12]	Fixed	No	Medium	Low
DRACD	Adaptive	Yes	Low	High

As shown in Table VII, the conventional method uses fixed thresholds and lacks adaptability, resulting in higher sensitivity to environmental variations. In contrast, DRACD employs adaptive thresholding and rolling reference updates, improving robustness and reducing false alarms. Minor deviation spikes may occur under abrupt illumination or viewpoint changes before stabilization.

The adaptive thresholding and controlled rolling update mechanism enable DRACD to maintain stable operation under environmental variations while preserving computational efficiency suitable for embedded UAV platforms.

VI. Conclusion

The limitations of static dual-reference change detection methods in UAV-based surveillance are addressed through the proposed lightweight Dual-Reference Adaptive Change Detection (DRACD) method. Conventional approaches relying on fixed thresholds and static references are highly sensitive to illumination changes, background complexity, and minor viewpoint variations, leading to false alarms and reduced reliability.

The proposed method introduces adaptive thresholding and a rolling reference update mechanism, enabling dynamic adjustment to gradual environmental changes while preserving computational efficiency. This allows the method to distinguish effectively between natural variations and actual anomalies.

Experimental results demonstrate that the proposed method significantly reduces false alarm rates under illumination variations and maintains reliable detection performance across different environments. A clear separation between normal and abnormal conditions is consistently observed, validating the robustness of the approach.

Furthermore, the method achieves these improvements without increasing computational complexity, making it suitable for real-time deployment on resource-constrained UAV platforms.

A potential limitation of the rolling reference update mechanism is that slowly evolving anomalies may be incorporated into the reference model if initially misclassified as normal. However, such situations are less likely under the considered UAV surveillance conditions and remain an area for future improvement.

Future work may focus on extending the method to handle more complex variations such as scale changes, rotation, significant viewpoint variations, and dynamic scene conditions.

REFERENCES

[1] G. Tang, J. Ni, Y. Zhao, Y. Gu, and W. Cao, "A survey of object detection for UAVs based on deep learning", *Remote Sensing*, vol. 16, no. 1, Art. no. 149, 2023.

[2] O. K. Pal, MD. S. H. Shovon, M. F. Mridha, and J. Shin, "In-depth review of AI-enabled unmanned aerial vehicles: trends, vision, and challenges", *Discover Artificial Intelligence*, vol. 4, Art. no. 97, 2024.

[3] X. Wu, W. Li, D. Hong, R. Tao, and Q. Du, "Deep learning for unmanned aerial vehicle-based object detection and tracking: A survey", in *IEEE Geoscience and Remote Sensing Magazine*, vol. 10, no. 1, pp. 91-124, 2022.

[4] Y. Han, C. Wang, and H. Luo, "LRDS-YOLO enhances small object detection in UAV aerial images with a lightweight and efficient design", *Scientific Reports*, vol. 15, Art. no. 22627, 2025.

[5] Y. Zhang, X. Chen, S. Sun, H You, Y. Wang, J. Lin, and J. Wang, "Vehicle detection in drone aerial views based on lightweight OSD-YOLOv10", *Scientific Reports*, vol. 15, Art. no. 25155, 2025.

[6] W. Li and Y. Zhang, "Enhanced small object detection in UAV aerial imagery through attention-gated backbone", *Scientific Reports*, vol. 16, Art. no, 2366, 2026.

[7] V. Kamath and A. Renuka, "Deep learning based object detection for resource constrained devices: A Systematic review", *Neurocomputing*, vol. 531, pp. 34–60, 2023.

[8] Q. Tan, Z. Du, and S. Chen, "Moving target detection based on background modeling and frame difference," *Proc. Comput. Sci.*, vol. 221, pp. 585–592, 2023.

[9] M. Yazdi and T. Bouwmans, "New trends on moving object detection in video images captured by a moving camera: A survey", *Computer Science Review*, vol. 28, pp. 157–177, 2018.

[10] B. Garcia-Garcia, T. Bouwmans, and A. J. R. Silva, "Background subtraction in real applications: Challenges, current models and future directions", *Computer Science Review*, vol. 35, Art. no. 100204, 2020.

[11] X. Fan, G. Wen, Z. Gao, J. Chen, and H. Jian, "An unsupervised moving object detection network for UAV videos", *Drones*, vol. 9, no. 2, Art. no. 150, 2025.

[12] K. S. Karreddula and A. K. Deb, "Detection of Normal and Abnormal Conditions for Boundary Surveillance using Unmanned Aerial Vehicle", *International Symposium of Asian Control Association on Intelligent Robotics and Industrial Automation (IRIA)*, pp. 50-56, 2021.

[13] S. Pal and A. K. Deb, "Linear parameter varying model-based predictive trajectory tracking control of quadrotor", *11th International Conference on Signal Processing and Integrated Networks* (*SPIN*), pp. 193-198, 2024.

[14] PX4 Development Team, "Pixhawk 4", *PX4 User Guide* [Online], Accessed 2026.

[15] Raspberry Pi Foundation, "Raspberry Pi 3 Model B+ Specifications", *Raspberry Pi Documentation* [Online], Accessed 2026.

[16] OmniVision Technologies, Inc., "OV5647 Color CMOS 5-Megapixel Camera with OmniBSI Technology", *Product Brief (Data Sheet)* [Online]. Accessed 2026.

[17] M. Din, A. Bashir, A. Basit, and S. Lakho, "Abandoned Object Detection using Frame Differencing and Background Subtraction", *International Journal of Advanced Computer Science and Applications*, vol. 11, no. 7, 2020.

[18] R. Ganapathyraja and S. P. Balamurugan, "A Comprehensive Analysis of Motion and Motionless Object Detection in Real Time Video Surveillance using Frame Difference and Background Subtraction", *Int. Conf. on Innov. Tech. and its Appl. in High. Edu.-Sci.*, pp. 45–51, 2022.